Mutual Inductance Measurement in Wireless Power Transfer Systems operating in the MHz range

Andrea Celentano, *Graduate Student Member, IEEE,* Carmine Paolino, *Graduate Student Member, IEEE,* Fabio Pareschi, *Senior Member, IEEE,* Luca Callegaro, Riccardo Rovatti, *Fellow, IEEE,* and Gianluca Setti, *Fellow, IEEE*

***Abstract*—This tutorial focuses on the problem of the experimental measurement of the mutual inductance (or, equivalently, of the coupling factor) of two coupled coils designed for a Wireless Power Transfer (WPT) system. Although many instruments and techniques are available for this purpose, in the literature, no clear guidelines defining the most reliable technique exist, and the vast majority of papers propose ad-hoc measurement approaches without clearly explaining pros and cons of each specific choice. The contribution of this paper is to fill this gap by i) reviewing the available methodologies that can be used to measure the mutual inductance, ii) highlighting the issues that may arise, and iii) identifying the most suitable technique for a particular use case. More specifically, to increase the impact of our analysis, we focus on the case of a couple of WPT coils for biomedical applications designed to work at 6.78 MHz, which is a setting both very common and quite tricky for the direct measurement.**

***Index Terms*—Mutual Inductance Measurement, Coupling Factor, Wireless Power Transfer.**

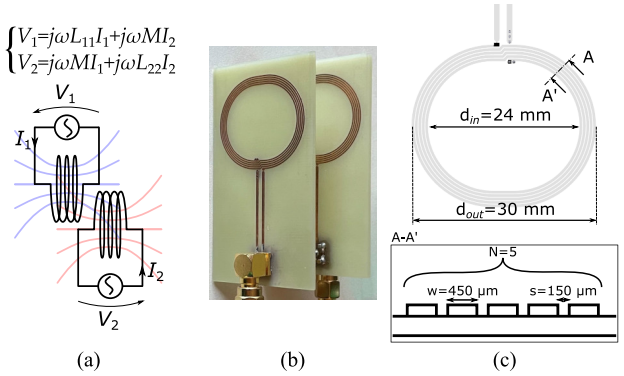

Fig. 1. (a) Two inductively coupled coils in a WPT system, mathematically described by the system of equations shown at the top. Assuming the two coils core-less and not perfectly aligned, the electromagnetic fluxes are not completely concatenated. (b) Picture of the two spiral PCB-printed coils used a reference case. (c) Geometrical characteristics of the coils.

I. Introduction

WIRELESS Power Transfer (WPT) systems gained increasing attention in recent years and in many areas. For biomedical applications, they represent a viable alternative to overcome issues deriving from the use of implanted batteries, i.e., size, longevity and bio-compatibility. Especially for systems where external and implanted devices are located in close proximity of each other, WPT relies on inductive coupling in which one coil is placed immediately outside the human body and the other inside it, giving rise to a near-field coupled inductance system.

The design of WPT system is always rather challenging. As an example, for biomedical applications [1]–[4], an immediate issue is related to the operating frequency trade-off. In fact, attenuation of the medium (e.g., the biological tissue between the coils) is roughly increasing with the operating frequency, and it is desirable to maintain it as low as possible. Conversely, the use of a high frequency is important to keep the coils sufficiently small to be easily implanted, especially for invasive applications, such as neurostimulators. One of the most common solutions for this trade-off is to set the nominal operating frequency within the ISM band centered at $6.78\,\mathrm{MHz}$ or $13.56\,\mathrm{MHz}$ [5], [6].

In these settings, the measurement of the self-inductance of the coils is usually simple. Conversely, the measurement of the mutual inductance M (or equivalently, of the coupling factor k) typically represents a tricky task, in particular for a loosely coupled coils system. The main problem, as detailed in the following, is due to the parasitic elements introduced by the measuring system, which are typically negligible with respect to the self-inductance value, but not with respect to the mutual inductance one.

Indeed, many reasons suggest that the mutual inductance M must be carefully evaluated, not only because it affects both the link gain and the load received power, but also because it features a strong sensitivity with respect both to the medium attenuation and to the coils distance and misalignment. If we also consider that many WPT systems are designed with resonant circuits [1], [7]–[10] whose behaviour strongly depends on all circuit parameters, the appropriate knowledge of M is even more fundamental. Of course, it is possible to base the

A. Celentano is with the Department of Electronics and Telecommunications, Politecnico di Torino, 10129 Torino, Italy (e-mail: andrea.celentano@polito.it).

C. Paolino is with the Nanolab, Advanced Technology Laboratory, ECE – Tufts University, 02155 Medford, MA, USA (e-mail: carmine.paolino@tufts.edu).

F. Pareschi is with the Department of Electronics and Telecommunications, Politecnico di Torino, 10129 Torino, Italy, and also with the Advanced Research Center on Electronic Systems (ARCES), University of Bologna, 40125 Bologna, Italy (e-mail: fabio.pareschi@polito.it).

L. Callegaro is with the Istituto Nazionale di Ricerca Metrologica (INRIM), 10135 Torino, Italy (e-mail: l.callegaro@inrim.it).

R. Rovatti is with the Department of Electrical, Electronic, and Information Engineering, University of Bologna, 40136 Bologna, Italy, and also with the Advanced Research Center on Electronic Systems (ARCES), University of Bologna, 40125 Bologna, Italy (e-mail: riccardo.rovatti@unibo.it).

G. Setti is with the CEMSE, King Abdullah University of Science and Technology (KAUST), Saudi Arabia (e-mail: gianluca.setti@kaust.edu.sa).

circuit design on the expected system parameters (including M) estimated by means of accurate electromagnetic simulation results. However, this may not take into account all parasitics and medium effects existing in a realistic environment. Due to all the above observations, the verification of the system characterization with direct measurement is of paramount importance [1], [11]–[13].

The main contribution of this tutorial is to tackle this issue by reviewing established methodologies for conducting such measurements while also shedding light on potential challenges that might emerge. As far as our understanding goes, the existing literature lacks such a comprehensive analysis. To make our analysis more practical, we focus on a case study of a couple of WPT coils for biomedical applications designed to operate at $6.78\,\mathrm{MHz}$ and around 100 mW [14].

This paper is organized as follows. In Section II the considered model for the coupled coils is proposed, and the state of the art about the available methodologies to measure M is explored. In Section III we perform the measurement of M on a coupled coils system built to work at $6.78\,\mathrm{MHz}$. In particular, we compare the direct measurement obtained with a Vector Network Analyzer (VNA) to the ones performed with an LCR meter. Finally, we draw the conclusion.

II. Coupled coils model and State of the art

Formally, when two (or more) coils are in proximity of each other, the magnetic field generated by one coil interferes with the other one(s), as sketched in Fig. 1(a). Modeling the system as a (loosely coupled) transformer may prove helpful in the analysis of the circuit [7], [8], [15]–[17].

In the phase-vector domain, and neglecting parasictics, one can write

$$\begin{aligned} V_1 &= j\omega L_{11} I_1 + j\omega M I_2 \\ V_2 &= j\omega M I_1 + j\omega L_{22} I_2 \end{aligned} \tag{1}$$

where M is the mutual inductance, L_{11} and L_{22} are the two self-inductances, and $V_{1(2)}$ and $I_{1(2)}$ are the phase vectors of the input (output) port voltages and currents. While L_{11} and L_{22} are constrained to be positive, M can be either positive or negative[1] according to an in-phase or out-of-phase coupling, respectively. The coupling factor k is defined as the dimensionless quantity $k = M/\sqrt{L_{11}L_{22}}$ and, similarly to what happens to M, it can assume a positive or negative value according to the coupling.

Eq. (1) is typically used for the sake of simplicity, thus keeping the underlying mathematical model as simple as possible. Indeed, the real behaviour is much more complex and results, if one wants to use (1), in each term of the model being a non-linear function of the frequency. In general, each parameter value is constant at low frequencies and rapidly increases around the so-called self-resonance frequency (SRF). As a consequence, inductances in (1) are generally described with a low-frequency value and by an SRF value that limits the validity range of the model.

[1]Actually, $M = 0$ is also acceptable, indicating that there is no interaction between the coils.

As already said, validation by means of real measurements of both the low-frequency values and of the SRF is fundamental. Yet, among all parameters in (1), the evaluation of M (i.e., both its low-frequency value and SRF) is more problematic since WPT systems are generally based on loosely coupled coils, with a relatively low value of M (i.e., $M^2 \ll L_{11}L_{22}$). The main problem here is that, when an instrument is set up for the correct measurement of L_{11} and L_{22}, its parasitics are kept negligible with respect to both L_{11} and L_{22}, but may strongly affect the measurement of M if k is small. Additionally, the measurement system may not be optimized for the desired frequency range.

In particular, operating frequencies commonly used in biomedical WPT systems represent a difficult setting as they are at the same time, too low for standard radio-frequency (RF) measurement techniques, and too high for low-frequency or quasi-stationary ones [18]. Yet, little or no attention is given in the literature to these aspects, and many papers can be found suggesting one method or another one [19], [20], without paying attention to their limitations.

Since the first mutual inductance modeling study [21], many results have been achieved both in modeling and measuring the mutual inductance of an inductive link [1], [12], [22]–[26]. Limiting ourselves to measurement techniques, and neglecting methods employed either in primary metrology (e.g., *three-voltmeter technique* [27]) or that need ad-hoc circuits (e.g., a compensation network in [28] or a whole resonant circuit in [29], [30]), the approaches known in the literature can be grouped into two main classes, according to the required measurement instrument:

a) approaches based on VNA and on the scattering matrix evaluation [19], [20], [31];
b) approaches based on LCR meter such as the series-antiseries technique [32], [33] (and the dual parallel-antiparallel one [32], not considered here due to space reasons), the direct measurement technique [34] and the one relying on the Z-matrix evaluation [35].

In the following, we detail these methodologies with the help of a reference case. The basic assumption for all these approaches is that the precision of the instrument is high enough to neglect error propagation in all measurement processing steps. Nevertheless, parasitics introduced either by the connection with the instrument ports or by the instrument itself limit the frequency application range of the approach.

III. A case study: Measurements on WPT coils for Biomedical Applications

We consider a system composed of two spiral-shaped printed circuit board (PCB) coils as in Fig. 1(b). The coils have been printed over a standard $1.6\,\mathrm{mm}$ board with FR4 substrate with a $35\,\mu\mathrm{m}$ copper plating, and are designed for a WPT system operating in the ISM band centered at $6.78\,\mathrm{MHz}$ (i.e., the nominal frequency adopted in many WPT systems) and around 100 mW (i.e., the typical power of inductive WPT biomedical implants). Each coil has an inductance of $L_{11} = L_{22} \approx 1.47\,\mu\mathrm{H}$ with a quality factor $Q \approx 50$ at the nominal frequency. The coils have been placed in front of

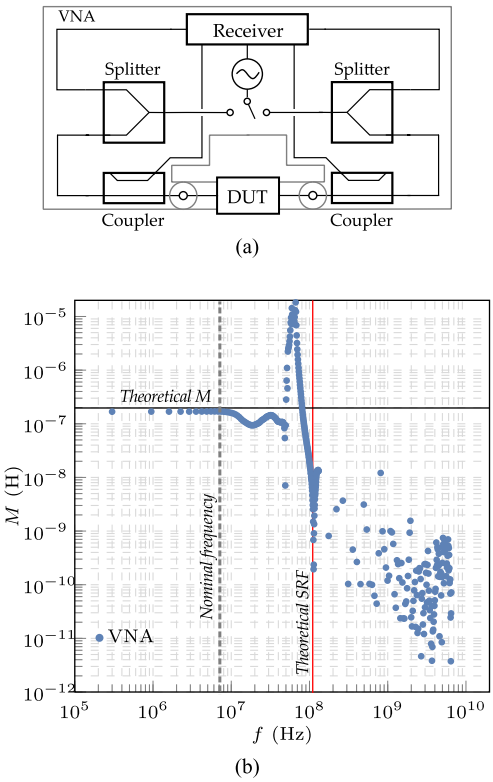

Fig. 2. (a) VNA basic block scheme. (b) VNA measurements obtained with a Keysight P9371A (blue dots). The black and red straight lines show the theoretical values of M and of the self-resonant frequency (SRF), respectively. The dashed gray line indicates the nominal working frequency.

each other at a nominal distance of $13.5\,\mathrm{mm}$, obtaining a 1:1 loosely coupled transformer. The geometrical properties of the coils are detailed in Fig. 1(c).

The theoretical electromagnetic model of this structure can be simply achieved with multiphysics software (e.g., ADS by Keysight and Q3D by Ansys) in which the 3D structure can be imported and simulated. Due to space constraints, we refer here to [1], where analytical results of the same structure are provided. Accordingly, M (at the nominal frequency and distance) results to be $\approx 153\,\mathrm{nH}$ ($k \approx 0.1$). Intrinsic parasitic capacitances set the theoretical SRF to be $\approx 110\,\mathrm{MHz}$. If however, for any reason, the electromagnetic simulation does not take into account all intrinsic parasitics, the theoretical SRF can result much higher than the real one. So, to validate the SRF and the M model, measurement is necessary. However, it is important to notice that even the introduction of parasitics in the measurement setup can result in a wrong measurement (and in particular of the SRF). Therefore, careful handling of both theoretical and measured results is required, and reasonable accurate conclusions are drawn when the theoretical and measured results overlap.

A. VNA measurements

The VNA is an electronic instrument that estimates the scattering matrix S by measuring the power of the incident and reflected waves. Once S is known, the Z matrix can be easily obtained by performing a simple S-to-Z conversion[2]. The values of L_{11}, L_{22} and M can then be obtained from the imaginary part of the Z matrix according to (1).

The simplified block diagram of a typical two-port VNA is shown in Fig. 2(a). A variable frequency signal waveform is generated within the VNA and it is delivered to the Device Under Test (DUT), assumed as a two-port circuit represented by the coaxial connectors in Fig. 2(a). The power of the incident and reflected waves at both ports of the DUT are alternately measured by toggling an internal switch, as illustrated in the figure. After the switch, the generated wave flows through a splitter, with the twofold purpose of providing a reference signal to the receiver and allowing the generated waveform to flow into the DUT. Additionally, two directional couplers are connected to both DUT ports. The first one collects the fraction of power that is reflected by the DUT. Instead, the power that passes through the DUT is collected by the second directional coupler. Matrix S is provided by the receiver, which compares, for both switch positions, the incident and reflected waveforms collected by the two couplers with the reference one coming from the splitter. To characterize two coupled coils by means of a VNA, one simply needs to connect each coil to a port and the instrument directly provides the corresponding S matrix. The main problem of this approach is that the majority of mid-price range VNAs are generally designed to correctly work at microwave frequencies: in the most common implementation, couplers are made by waveguides that resonate in a suitable RF range, only. Hence, it is quite difficult to get high accuracy measurements in the ISM band centered either at $6.78\,\mathrm{MHz}$ or $13.56\,\mathrm{MHz}$. Notwithstanding the above issue, several works in the literature suggest this approach, irrespective of the WPT application and frequency of operation [19], [20].

Measurements of M for the case-study system by means of the Keysight P9371A VNA are shown in Fig. 2(b) in the whole frequency range of operation for the instrument as declared by the manufacturer, i.e. $[300\,\mathrm{kHz}, 6.5\,\mathrm{GHz}]$[3].

Experimentally, measurements are in quite good agreement with the theoretically expected results at low frequencies (up to approximately $5\,\mathrm{MHz}$), but matching becomes quite poor before approaching the SRF frequency either because some parasitics are not taken into account in the analytical model or because of the introduction of parasitics by the instrument (or the instrument setup) itself.

B. LCR meter measurements

The LCR meter, also known as *bridge*, is specifically designed for the low-frequency measurement of impedances with arbitrary phase angles. The impedance definition employed by the bridge is dependent on its accuracy class, the best one of which uses a 4-port one [36]. As a matter of fact, the four terminal-pair impedance definition is the most complete one used in electrical metrology. The four ports are generally labeled as High Current (HC), High Potential (HP), Low Potential (LP), and Low Current (LC).

[2]The characteristic impedance Z_0 of the line is the only extra parameter needed for the conversion.

[3]Notice that, despite the wide bandwidth, the VNA manufacturer does not provide any accuracy details below $10\,\mathrm{MHz}$.

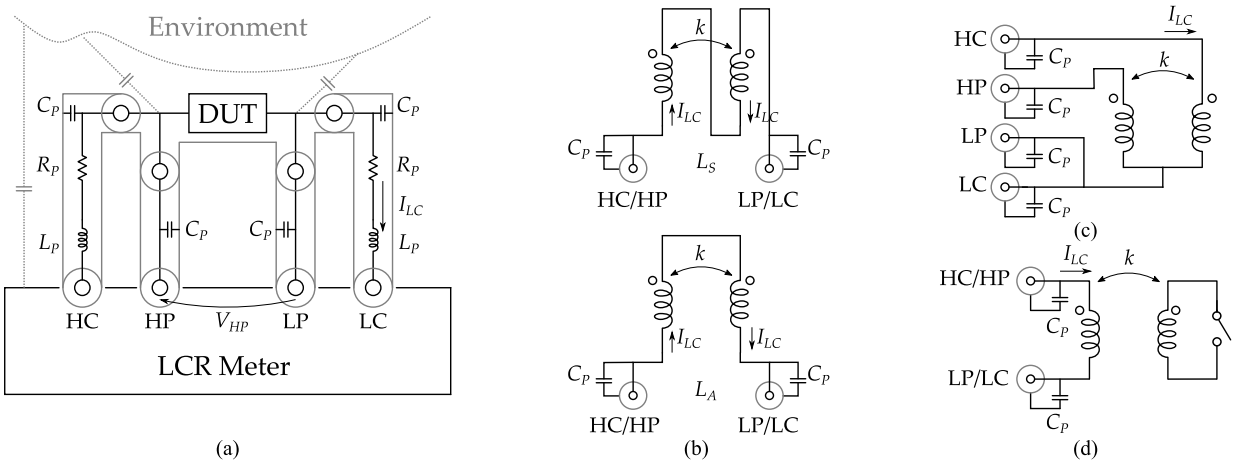

Fig. 3. (a) LCR basic block scheme. (b) LCR indirect method: series (L_S) and anti-series (L_A) configuration. (c) Direct method for the measurement of M, consisting in a single self-inductance measurement. (d) Z-matrix method for the measurement of M, consisting in three 1-port measurements of the impedances Z_{1o2}, Z_{2o1} and either Z_{1s2} or Z_{2s1}.

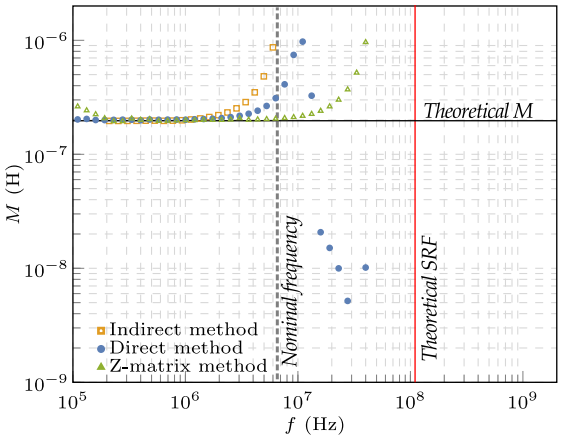

Fig. 4. LCR measurements performed according to the three different considered methodologies. The indirect method (in yellow) is performed by means of an HP 4192A. The direct method (in blue) and the Z-method (in green) are performed by means of an Agilent 4294A. The black and red straight lines show the theoretical values of M and of the self-resonant frequency (SRF), respectively. The dashed gray line indicates the nominal working frequency.

An external *fixture* is typically required for being able to connect the DUT to the four LCR ports. As an example, the typical connection of a 2-terminal DUT to a 4-port LCR meter is shown in Fig. 3(a). The four ports are assumed to be coaxial pairs, and the shield is highlighted in grey in the figure. The DUT is excited by injecting a current at port HC, which is measured as I_{LC} at port LC. Conversely, no current is flowing through ports HP and LP, which are used to measure the voltage at the DUT by imposing $V_{\mathrm{LP}} = 0$ and by measuring the voltage V_{HP} at port HP. The impedance of the DUT is then computed as $Z = V_{\mathrm{HP}}/I_{\mathrm{LC}}$.

Thanks to this definition, the LCR meter is able to reject the influence of both the stray resistances and stray inductances labeled as R_P and L_P in Fig. 3(a), respectively. Furthermore, also the stray capacitances C_P introduced either by the LCR meter or by the fixture do not theoretically influence the measurement. Capacitances at the HP and HC ports are both driven by the current injected at the HC port and have no influence on I_{LC} and V_{HP}, whereas the ones at the LP and LC ports are virtually shorted by the LCR internal feedback [32]. Additionally, parasitics can be compensated by means of OPEN, SHORT, and LOAD corrections, available on high-end instruments [34]. Performance is limited at high frequency by the parasitic capacitances between the DUT and the environment.

As already mentioned, this technique can be employed to perform different kinds of mutual inductance measurements which are described in detail in the following.

1) Indirect method (Series/Antiseries): the mutual inductance can be indirectly derived from the direct measurement of the self-inductance in the series and antiseries configurations shown in Fig. 3(b). Since the series connection leads to $L_S = L_{11} + L_{22} + 2M$, and the antiseries one leads to $L_A = L_{11} + L_{22} - 2M$, the mutual inductance can be calculated as $M = (L_S - L_A)/4$. An equivalent dual measurement approach exploiting a parallel-antiparallel is also possible, but it is not considered here.

Measurements obtained with the 5 Hz-to-13 MHz Keysight/Hewlett-Packard 4192A Impedance Analyzer are shown as the yellow squares in Fig. 4 together with the indication of the theoretical M value (dark solid line) and SRF (red solid line). The inductance measurements at low frequency are in good agreement with the expected value, but the resonance is observed at a frequency much lower than the expected one, as low as the 6.78 MHz operating frequency we are interested in (dashed gray line). As a matter of fact, the upper validity limit of this approach barely goes above one MHz.

The limitation of this methodology is due to the inductances and the stray capacitances of the two (different) custom fixtures required to connect the two coils in the series (to measure L_S) and antiseries (to measure L_A) configuration. The problem is twofold. On the one hand, being the fixtures different (a different connection is required), the parasitics

are also different and do not compensate when computing $L_S - L_A$. On the other hand, it is not possible to force the compensation by means of the OPEN, SHORT, and LOAD correction capabilities, as these states are well defined for a single impedance, but not for a connection of more impedances.

2) Direct method: by connecting the coupled coils as shown in Fig. 3(c), the mutual inductance value is directly obtained from the self-inductance measurement of the shown topology. As a matter of fact, when the test current flows from HC through the primary winding, the secondary voltage is measured at HP so that $V_{\mathrm{HP}} = j\omega M \cdot I_{\mathrm{LC}}$.

Measurements in this configuration have been taken with a Keysight/Agilent 4294A Precision Impedance Analyzer, with $110\,\mathrm{MHz}$ upper frequency limit, which is much higher than the previously considered one. Results are shown as the blue circles in Fig. 4 and are clearly not very different from those observed in the previous case.

The main problem of this method is given by the stray capacitance seen at the HP port, that is virtually connected in parallel to the inductance M. In fact, in this configuration, the instrument forces a current I_{LC} flowing in one coil (i.e., the one connected to HC), but it does not inject any current in the other coil (i.e., the one connected to HP). As a consequence, C_P at the HP port is charged by the current due to the concatenated flux, by therefore altering V_{HP} and the measurement of M.

The expected result is the anticipation of the SRF, which is shown in Fig. 4. The upper frequency limit of this approach is slightly higher, but still comparable, to what was observed in the previous case, despite the larger bandwidth of the considered instrument.

3) Z-matrix method: this method is very similar to that adopted by Suzuki in [37] for calibrating four-terminal pairs admittance standards and the measurement of Z was achieved by adopting one-port VNA measurements, only. The very same procedure can be applied also to LCR meters as in Fig. 3(d), and consists in three (or four) one-port measurements $Z_{1\mathrm{o}2}$, $Z_{2\mathrm{o}1}$, $Z_{1\mathrm{s}2}$ and/or $Z_{2\mathrm{s}1}$. The notation $Z_{1\mathrm{o}2}$ ($Z_{2\mathrm{o}1}$) indicates the impedance at the primary (secondary) port when the secondary (primary) is open-circuited, whereas $Z_{1\mathrm{s}2}$ ($Z_{2\mathrm{s}1}$) indicates the impedance at the primary (secondary) port when the secondary (primary) is short-circuited. Note that $Z_{1\mathrm{o}2} = j\omega L_{11}$ and $Z_{2\mathrm{o}1} = j\omega L_{22}$ in (1). The value of M is derived in [35] by directly applying the Z-matrix definition to a two-port circuit, and can be easily demonstrated to be $M = \sqrt{(Z_{1\mathrm{s}2} - Z_{1\mathrm{o}2}) \cdot Z_{2\mathrm{o}1}}/\omega$ or $M = \sqrt{(Z_{2\mathrm{s}1} - Z_{2\mathrm{o}1}) \cdot Z_{1\mathrm{o}2}}/\omega$.

Measurements with this approach have been performed by means of the Keysight/Agilent 4294A. Results are shown as the green triangles in Fig. 4. With respect to the two previously considered cases the range of validity of the measurements is almost one order of magnitude higher, even though we are still quite far from the expected $110\,\mathrm{MHz}$ SRF[4].

The advantage of this methodology lies in its simplicity as it reduces in evaluating the Z matrix of a two-port circuit through one-port measurements only, enabling the capacity of parasitic corrections allowed by high-end instrumentation. Furthermore, no additional fixtures are required (which were conversely necessary in the series/antiseries case), limiting the introduction of parasitic elements. This is the reason why this approach has been shown to be the most reliable one. Measurements are in agreement with the theoretical expected results up to approximately $20\,\mathrm{MHz}$.

[4]Measuring such value would indeed not be possible with the Keysight/Agilent 4294A as it coincides with the upper limit of the instrument bandwidth.

TABLE I
COMPARISON OF THE EXAMINED METHODOLOGIES

Instrument	VNA	LCR		
Methodology		Indirect	Direct	Z-matrix
Model	Keysight P9371	HP 4192A	Agilent 4294A	Agilent 4294A
# of Meas.	one	two	one	two
Validity up to	$\approx 5\,\mathrm{MHz}$	$\approx 1\,\mathrm{MHz}$	$\approx 10\,\mathrm{MHz}$	$\approx 20\,\mathrm{MHz}$
Ad hoc fixture	no	yes	yes	no

For the sake of clarity, all the main characteristics of the analyzed methodologies are summarized in Table I.

IV. CONCLUSION

In this paper, we have reviewed the available methodologies that can be in principle used to measure the mutual inductance of coupled coils in WPT applications that adopt either the VNA or the LCR meter. It is important to note that our intention was not to assert which techniques can be universally employed and deemed superior to others, but rather to comprehensively understand the potential issues that can arise during these measurements. This knowledge can be used to carefully interpret the results and helps to understand the most appropriate methodology for a given case study. We have shown that mid-price range VNAs do not always provide accuracy details below a certain frequency, although they can outperform some techniques employing the LCR meter. Despite limitations in LCR-meter methodologies, the Z-matrix method stands out as the most suitable technique both for its simplicity and validity in a wider frequency range.

REFERENCES

[1] M. Schormans, V. Valente, and A. Demosthenous, "Practical Inductive Link Design for Biomedical Wireless Power Transfer: A Tutorial," *IEEE Trans. Biomed. Circuits Syst.*, vol. 12, no. 5, pp. 1112–1130, Oct. 2018. doi: 10.1109/TBCAS.2018.2846020

[2] J. Lee *et al.*, "Wireless Power Transfer for Small Implantable Devices by using Smartphones with Relay Coils," in *Intern. Symp. on Antennas and Prop. and North American Radio Sc. Meeting*, Jul. 2020, pp. 1395–1396. doi: 10.1109/IEEECONF35879.2020.9329551

[3] S. S. Biswal, D. P. Kar, S. K. Samal, and S. Bhuyan, "Investigation of correlation of design parameters in wireless power transfer system," *IET sci. meas. technol.*, vol. 15, no. 5, pp. 427–433, Jul. 2021. doi: 10.1049/smt2.12043

[4] S. Stoecklin, A. Yousaf, T. Volk, and L. Reindl, "Efficient Wireless Powering of Biomedical Sensor Systems for Multichannel Brain Implants," *IEEE Trans. Instrum. Meas.*, vol. 65, no. 4, pp. 754–764, Apr. 2016. doi: 10.1109/TIM.2015.2482278

[5] Y. Jia *et al.*, "A mm-Sized Free-Floating Wirelessly Powered Implantable Optical Stimulation Device," *IEEE Trans. Biomed. Circuits Syst.*, vol. 13, no. 4, pp. 608–618, Aug. 2019. doi: 10.1109/TBCAS.2019.2918761

[6] B. Lee *et al.*, "An Inductively-Powered Wireless Neural Recording and Stimulation System for Freely-Behaving Animals," *IEEE Trans. Biomed. Circuits Syst.*, vol. 13, no. 2, pp. 413–424, Apr. 2019. doi: 10.1109/TBCAS.2019.2891303

[7] A. Celentano *et al.*, "A Comparison between Class-E DC-DC Design Methodologies for Wireless Power Transfer," in *Inter. Midwest Symp. on Circ. and Systems*, Aug. 2021, pp. 71–74. doi: 10.1109/MWSCAS47672.2021.9531712

[8] T. Nagashima *et al.*, "Steady-state analysis of isolated class-e^2 converter outside nominal operation," *IEEE Trans. Ind. Electron*, vol. 64, no. 4, pp. 3227–3238, Apr. 2017. doi: 10.1109/TIE.2016.2631439

[9] J. Liu, G. Wang, G. Xu, J. Peng, and H. Jiang, "A Parameter Identification Approach With Primary-Side Measurement for DC–DC Wireless-Power-Transfer Converters With Different Resonant Tank Topologies," *IEEE Trans. Transp. Electrific.*, vol. 7, no. 3, pp. 1219–1235, Sep. 2021. doi: 10.1109/TTE.2020.3048026

[10] M. Kiani, "Wireless Power Transfer and Management for Medical Applications: Wireless power," *IEEE Solid-State Circuits Mag.*, vol. 14, no. 3, pp. 41–52, 2022. doi: 10.1109/MSSC.2022.3178671

[11] D. Lin, J. Yin, and S. Y. R. Hui, "Parameter identification of wireless power transfer systems using input voltage and current," in *Energy Conv. Cong. and Exposition*, Sep. 2014, pp. 832–836. doi: 10.1109/ECCE.2014.6953483

[12] W. G. Hurley *et al.*, "A Unified Approach to the Calculation of Self- and Mutual-Inductance for Coaxial Coils in Air," *IEEE Trans. Power Electron.*, vol. 30, no. 11, pp. 6155–6162, Nov. 2015. doi: 10.1109/TPEL.2015.2413493

[13] S. Liu *et al.*, "Contactless Measurement of Current and Mutual Inductance in Wireless Power Transfer System Based on Sandwich Structure," *IEEE J. Emerg. Sel. Topics Power Electron.*, vol. 10, no. 5, pp. 6345–6357, Oct. 2022. doi: 10.1109/JESTPE.2022.3188641

[14] A. Trigui, S. Hached, A. C. Ammari, Y. Savaria, and M. Sawan, "Maximizing Data Transmission Rate for Implantable Devices Over a Single Inductive Link: Methodological Review," *IEEE Rev. Biomed. Eng.*, vol. 12, pp. 72–87, 2019. doi: 10.1109/RBME.2018.2873817

[15] A. Celentano *et al.*, "A Wireless Power Transfer System for Biomedical Implants based on an isolated Class-E DC-DC Converter with Power Regulation Capability," in *63rd Intern. Midwest Symp. on Circ. and Systems*, Aug. 2020, pp. 190–193. doi: 10.1109/MWSCAS48704.2020.9184689

[16] W. Zhang, J. C. White, A. M. Abraham, and C. C. Mi, "Loosely Coupled Transformer Structure and Interoperability Study for EV Wireless Charging Systems," *IEEE Transactions on Power Electronics*, vol. 30, no. 11, pp. 6356–6367, Nov. 2015. doi: 10.1109/TPEL.2015.2433678

[17] A. Bharadwaj, A. Sharma, and C. C. Reddy, "An Unconventional Measurement Technique to Estimate Power Transfer Efficiency in Series–Series Resonant WPT System Using S-Parameters," *IEEE Trans. Instrum. Meas.*, vol. 71, pp. 1–9, 2022. doi: 10.1109/TIM.2022.3181291

[18] L. Callegaro, "The metrology of electrical impedance at high frequency: a review," *Meas. Sci. Technol.*, vol. 20, no. 2, p. 022002, Feb. 2009. doi: 10.1088/0957-0233/20/2/022002

[19] A. Ariffin, A. Mori, and M. Inamori, "Analyzation of antenna measurement method for wireless power transmission," in *IEEE Region 10 Conference*, Nov. 2017, pp. 219–222. doi: 10.1109/TENCON.2017.8227865

[20] S.-J. Jeon and D.-W. Seo, "Coupling Coefficient Measurement Method with Simple Procedures Using a Two-Port Network Analyzer for a Multi-Coil WPT System," *Energies*, vol. 12, no. 20, p. 3950, Oct. 2019. doi: 10.3390/en12203950

[21] F. Grover, "The Calculation of the Mutual Inductance of Circular Filaments in Any Desired Positions," *Proceedings of the IRE*, vol. 32, no. 10, pp. 620–629, Oct. 1944. doi: 10.1109/JRPROC.1944.233364

[22] M. Al-Saadi, S. Valtchev, J. Gonçalves, and A. Crăciunescu, "New Analytical Formulas for Coupling Coefficient of Two Inductively Coupled Ring Coils in Inductive Wireless Power Transfer System," in *Green Energy and Networking*, X. Jiang and P. Li, Eds. Springer International Publishing, 2020, vol. 333, pp. 117–127. ISBN 978-3-030-62482-8

[23] Z. Li and M. Zhang, "Mutual inductance calculation of circular coils arbitrary positioned with magnetic tiles for wireless power transfer system," *IET Power Electron.*, vol. 13, no. 16, pp. 3522–3527, Dec. 2020. doi: 10.1049/iet-pel.2020.0392

[24] T. Liu, Z. Wei, H. Chi, and B. Yin, "Inductance Calculation of Multilayer Circular Printed Spiral Coils," *J. Phis.:Conf. Ser.*, vol. 1176, p. 062045, Mar. 2019. doi: 10.1088/1742-6596/1176/6/062045

[25] A. O. Amos, H. Ykandar, A. Yasser, and D. Karim, "Computation of the mutual inductance between circular filaments with coil misalignment," in *Africon*, Sep. 2013, pp. 1–5. doi: 10.1109/AFRCON.2013.6757626

[26] J. Acero *et al.*, "Analysis of the Mutual Inductance of Planar-Lumped Inductive Power Transfer Systems," *IEEE Trans. Ind. Electron.*, vol. 60, no. 1, pp. 410–420, Jan. 2013. doi: 10.1109/TIE.2011.2164772

[27] J. Bohacek, T. Jursa, and R. Sedlacek, "Calibrating Standards of Mutual Inductance," in *Instrumen. Meas. Tech. Conf. Proceedings*, vol. 2, 2005, pp. 1002–1004. doi: 10.1109/IMTC.2005.1604289

[28] Z. Li *et al.*, "A Compensation Method to Measure the Mutual Inductance at Low Frequency," *IEEE Trans. Instrum. Meas.*, vol. 60, no. 7, pp. 2292–2297, Jul. 2011. doi: 10.1109/TIM.2010.2099270

[29] S. Raju, M. Chan, and C. P. Yue, "Modeling of an inductive link for wireless power applications," in *Intern. Conf. of Electron Devices and Solid-state Circ.*, Jun. 2013, pp. 1–2. doi: 10.1109/EDSSC.2013.6628105

[30] W. Sokhui, Y. Dongsheng, T. Jiangwei, C. Zixin, and J. Songnam, "A Mutual Inductance Measurement Method for the Wireless Power Transfer System," *IOP Conf. Ser.: Mater. Sci. Eng.*, vol. 486, p. 012146, Jul. 2019. doi: 10.1088/1757-899X/486/1/012146

[31] J. Blanc, "A Simple Technique for Characterization of WPT Coils," in *Wireless Power Transfer Conf.*, Jun. 2018, pp. 1–4. doi: 10.1109/WPT.2018.8639126

[32] L. Callegaro, *Electrical impedance principles, measurement, and applications*. Boca Raton, Fla.: CRC Press, 2013. ISBN 978-1-4398-4910-1

[33] C. Shi, S. Lee, S. S. Aguilar, and E. Sánchez-Sinencio, "A Time-Domain Digital-Intensive Built-In Tester for Analog Circuits," *Journal of Electronic Testing*, vol. 34, no. 3, pp. 313–320, Jun. 2018. doi: 10.1007/s10836-018-5713-1

[34] *Impedance Measurement Handbook. A guide to measurement technology and techniques*, 4th ed. Keysight Technologies, 2014.

[35] S. Hackl, C. Lanschutzer, P. Raggam, and W. Randeu, "A novel method for determining the mutual inductance for 13.56MHz RFID systems," in *Intern. Symp. on Comm. Sys., Networks and Digital Sig. Process.*, Jul. 2008, pp. 297–300. doi: 10.1109/CSNDSP.2008.4610726

[36] R. D. Cutkosky, "Four-terminal-pair networks as precision admittance and impedance standards," *IEEE Trans. Comm. Electron.*, vol. 83, no. 70, pp. 19–22, Jan. 1964. doi: 10.1109/TCOME.1964.6539563

[37] K. Suzuki, "A new universal calibration method for four-terminal-pair admittance standards," *IEEE Trans. Instrum. Meas.*, vol. 40, no. 2, pp. 420–422, Apr. 1991. doi: 10.1109/TIM.1990.1032975